WARSAW UNIVERSITY OF TECHNOLOGY Index 351733
FACULTY OF CIVIL ENGINEERING
COMMITTEE FOR CIVIL AND WATER ENGINEERING
POLISH ACADEMY OF SCIENCES ISSN 1230-2945
DOI: 10.24425/ace.2024.150970
ARCHIVES OF CIVIL ENGINEERING
Vol. LXX ISSUE 3 2024
pp. 57 –69

Research paper

Construction and simulation of a decision model for anti-slip restoration technology of asphalt pavement surface based on vehicle dynamics

Rui Cheng[1], Xinkai Li[2], Lichao Wang[3]

Abstract: Taking real-time and effective preventive maintenance measures on in-service roads can reduce traffic congestion, eliminate potential road safety hazards, and greatly reduce road maintenance costs. Therefore, based on the Persson friction theory, this study first determines the evaluation indicators for the anti slip ability of asphalt pavement. And based on vehicle dynamics and contact friction between tires and road surface, the anti-skid thresholds of road surfaces for different road conditions and vehicle models are solved through simulation. This study utilizes Python and neural network algorithms to establish a decision-making model for anti-slip recovery technology of asphalt pavement. The experiment shows that the model trained by Back Propagation neural network has high accuracy. The training accuracy of the model is stable at around 0.90, and the training loss value is around 0.34, which can be used for decision-making in anti slip recovery technology. When the speed is less than 60 km/h, the increase in the threshold of dynamic friction coefficient is significant. The maximum difference in growth rate is 47.9%. When the speed exceeds 60 km/h, the increase in the threshold of dynamic friction coefficient gradually slows down. Therefore, at lower speeds, it is more essential to consider the variable value of the dynamic friction coefficient. When the speed is high, more consideration needs to be given to its reference value. This study provides a scientific basis for ensuring that the anti slip ability of the road surface always meets the requirements of driving safety, and has important engineering practical value, economic and social benefits.

Keywords: Persson's friction theory, vehicle dynamics, road, antiskid, asphalt, BP, decision

[1]MsC., Heilongjiang Transportation Planning and Design Research Institute Group Co., Ltd., Harbin 150090, China, e-mail: chengr2023@126.com, ORCID: 0009-0003-3361-3671

[2]Ph.D., School of Transportation Science and Engineering, Harbin Institute of Technology, Harbin 150090, China, e-mail: lxkhit@126.com, ORCID: 0009-0003-7385-332X

[3]MsC., Heilongjiang Jiaotou Highway Construction Investment Co., Ltd., Harbin 150090, China, e-mail: wanglichao202308@163.com, ORCID: 0009-0000-7829-7308

1. Introduction

According to statistics from the transportation department over the years, highways have transitioned from high-speed construction to management and maintenance. The timely restoration of road structure and function will become a research hotspot [1]. Effectively applying preventive maintenance measures can greatly reduce the workload of large and medium-sized road repairs, and reduce traffic closures and congestion caused by maintenance [2]. At present, asphalt pavement maintenance strategies often focus on intuitive road surface diseases such as ruts and potholes, and pay insufficient attention to the impact of road surface anti slip performance. Especially in rainy and snowy weather, the frequent occurrence of traffic accidents in tunnels and long downhill sections is closely related to the insufficient skid resistance of the road surface [3]. Therefore, using anti-slip ability as an important reference factor for determining the timing and effectiveness of preventive maintenance of asphalt pavement has great practical significance [4]. With the rapid development of computer technology, efficient and reliable modern algorithms such as genetic algorithms, reinforcement learning, and artificial neural networks have been applied to road maintenance management. Among them, backpropagation neural networks (BPNN) have strong computing power. It calculates the corresponding labels through the input of features, which is very consistent with the anti slip maintenance decision [5]. This study innovatively established the anti-slip index of asphalt pavement built on the dynamic friction coefficient (DFC) between vehicle tires and the road surface. And based on vehicle dynamics software and BPNN, a decision-making model for anti slip recovery technology of asphalt pavement has been established. The goal of this paper is to give real-time and fast anti slip performance maintenance and recovery decisions for in-service asphalt roads.

2. Related works

With the gradual improvement of the road traffic network, road construction is gradually transitioning towards management and maintenance. The timely maintenance and repair of in-service roads has gradually become a key topic in the field of transportation both domestically and internationally. Researchers such as Wang et al. established a vehicle dynamics model in the vehicle dynamics software Carsim and designed an algorithm for estimating the friction state between tires and road surfaces based on tire angular velocity information. This method can effectively estimate the state changes of tire road friction and the speed of the vehicle [6]. Hu and other scholars proposed a two-stage estimation scheme based on tire road friction coefficient estimation of longitudinal vehicle dynamics, which limits the interference of vehicle motion. This scheme has high accuracy in estimating road friction and low impact on vehicle speed [7]. Furlan and Mavros conducted simulation tests on vehicles on several road surfaces based on the Persson's friction theory. They proposed a model that combines artificial neural network configuration with tire models. The running speed of this research model has been greatly improved, which can effectively predict the peak friction and the gradual reduction of tire force [8]. Scholars such as Pérez Acebo et al. established a short-term model that

only considers surface materials, annual average daily traffic volume, and lanes, as well as a long-term model with polishing threshold values, by collecting data on the minimum friction values of summer road surfaces. This model has high predictive performance for the minimum slip resistance of highways [9].

Scholars such as Correa et al. have found through their research on the maintenance issues of real network level asphalt pavement that the Analytic Hierarchy Process performs better than other methods in comparing a large number of different maintenance strategies and determining maintenance priorities [10]. Mahmood and other experts have established a multi input unified prediction model based on artificial neural networks based on numerical and mixed classification features of in-service road test sections in the United States. The results indicate that the research model provides a high correlation between observed and predicted deterioration during the training phase [11]. Jing et al. proposed a calculation method for the quality recovery index of recycled pavement, and used the Analytic Hierarchy Process to calculate the index weight. At the same time, a comprehensive decision-making evaluation system was designed. Research has shown that the weight of the pavement quality recovery index is the highest [12]. Wei et al. proposed a parallel multi-scale method based on random aggregate generation to address the issue of the fact that the asphalt concrete (AC) layer in asphalt pavement is heterogeneous and cannot truly reflect the complex mechanical behavior of the pavement. Experiments have shown that rising the AC layer thickness can low down the stress at the top of the AC layer on the road surface at low temperatures [13].

In summary, the current evaluation indicators are mostly superficial measurement indicators, which fail to start from the friction mechanism between tires and the road surface, and insufficient consideration is given to the road texture. The reliability and efficiency of measurement indicators are not high, resulting in poor maintenance effectiveness of asphalt pavement. Therefore, this study starts from the texture characteristics of APS, selects reasonable anti slip evaluation indicators based on the friction mechanism between tires and pavement, and constructs a decision-making model for anti slip recovery technology of APS.

3. Construction method of decision model for APS slip restoration technology based on vehicle dynamics

This study starts from directly providing pavement texture information of tire to road friction, and selects evaluation indicators for the anti slip ability of asphalt pavement. Then, the anti-slip recovery ability of different preventive maintenance measures for asphalt pavement is compared. Based on vehicle dynamics and contact friction between tires and road surface, through simulation experiments, the anti-slip thresholds of road surfaces for different road conditions and vehicle models are solved. A decision model for anti-slip recovery technology of asphalt pavement has been established using Python and neural network algorithms.

3.1. Construction of a calculation model for DFC between tire and road surface based on persson friction theory

The Persson theory has a high degree of compatibility with the interaction between tires and road surfaces, fully reflecting the actual contact state between the two [14]. The micro and macro textures directly affect the anti slip performance of asphalt pavement, and are also the key considerations for anti slip recovery. When the vehicle speed is low, the micro texture provides the main anti slip effect [15]. Macro texture plays a major role in road drainage and anti slip at high vehicle speeds. In addition, according to the average level of the cross-section of the road texture, it can be divided into positive and negative textures. From a statistical perspective, asphalt pavement has typical self similarity [16]. This study adopts the most representative Hausdorff dimension. Its expression is Equation (3.1).

$$N(r) \propto r^{-D_H} \quad \text{or} \quad D_H = \ln N(r) / \ln\left(\frac{1}{r}\right) \tag{3.1}$$

In Equation (3.1), D_H stands for Hausdorff dimension, H stands for Hurst index. $N(r)$ represents the number of dimensions, and r represents the fractal dimension scale. Due to the fact that asphalt pavement is not a perfect self similar surface, its self similarity is established within a certain range. Assuming that the self similarity of asphalt pavement is established at wavelength $\lambda \in (\lambda_0, \lambda_1)$, the lower limit value λ_0 of its wavelength texture is at the micrometer level. The upper limit value λ_1 is the nominal maximum particle size of the asphalt mixture aggregate. Assuming that the contribution of asphalt pavement to the hysteresis force under different dimensions is only related to λ/h. h is the height above the average surface of the road texture, approximately equal to the amplitude of the positive texture. Under dry conditions, positive textures contribute more to the friction coefficient than negative textures. Based on this, Persson explored the hysteresis phenomenon of rubber under different magnifications. Taking into account factors such as adhesion and hysteresis, surface power spectrum is used to express the surface roughness of asphalt pavement [17]. In the typical power spectrum of asphalt pavement, the slope is related to the fractal index of the surface, as expressed by Equation (3.2).

$$C(q) \sim q^{-2(H+1)} \tag{3.2}$$

In Equation (3.2), when the proportion coefficient in the x, y direction is ζ, to achieve uniform statistical characteristics on the surface, the proportion coefficient along the z-direction is Υ^H. It has a relationship $H = 3 - D_f$ with the fractal dimension D_f, and the power spectrum smaller than q_0 is approximately constant. When the tire interacts with the road surface, the deformation of the tire can be decomposed into three directions: x, y, and z. Based on the theory of viscoelastic mechanics, using DFT to convert it into a frequency function indicates that the distribution response displacement field corresponding to the direction is Equation (3.3).

$$u_i(q, \omega) = \frac{1}{(2\pi)^3} \int \mathrm{d}^2 x \mathrm{d}t u_i(x, t) e^{-i(q \cdot x - \omega t)} \tag{3.3}$$

Due to $\sigma_i(q,\omega) \approx u_i(q,\omega)$, the stress-strain relationship can be established as shown in Equation (3.4).

$$u(q,\omega) = M(q,\omega)\,\sigma(q,\omega) \tag{3.4}$$

In Equation (3.4), $M(q,\omega)$ represents the flexibility matrix. Considering the hysteresis effect caused by the interaction between the tire and the road surface, the elastic modulus has the following expression (3.5).

$$(M)^{-1} = -Eq/2(1-v)^2 \tag{3.5}$$

Through a series of formulas, the expression of the DFC between the tire and road surface based on the Persson friction theory is finally obtained, as shown in Equation (3.6).

$$\mu = \frac{1}{4\pi}(q_0 h_0)^2 \left(\int_{\frac{q_L}{q_0}}^{1} \mathrm{d}\zeta \zeta^3 P(q_0\zeta) + \int_{1}^{\frac{q_L}{q_0}} \mathrm{d}\zeta \zeta^{-2H+1} P(q_0\zeta) \right) \times \int_0^{2\pi} \mathrm{d}\phi Im \frac{E(q_0\zeta v\cos\phi)}{(1-\gamma^2)\sigma_0} \tag{3.6}$$

In Equation (3.6), σ_0 represents the vertical compressive stress. Using appropriate methods to quickly and accurately obtain the texture of asphalt pavement is crucial for solving friction coefficients and evaluating anti slip performance. Currently, the Close Range Photogrammetry system (CRP) in non-contact measurement is the most widely used and has high measurement accuracy. In addition, based on the CRP method, the Automatic close range photogrammetry system (ACRP system) has also been developed. The paper is based on the VisualSFM open-source framework and implements reverse reconstruction of point clouds through programming. And the generated point cloud can be registered using the nearest point iteration method. From the perspective of road surface skid resistance, the driving safety of automobiles is mainly evaluated from aspects such as braking distance, whether there is sideslip during driving, and whether there is rollover. The study adopts the critical safe distance model proposed by scholars such as Zhong Yong, as shown in Equation (3.7) [18].

$$S_{\text{safe}} \geq 0.36(V_b - V_a) + 0.33V_b + \frac{(V_b - V_a)(V_b + V_a)}{25.92 j_{\max}} \tag{3.7}$$

In Equation (3.7), V_a, V_b represents the front and rear vehicle speeds (km/h), respectively. $j_{\max}$ represents the maximum continuous deceleration. Based on the threshold of DFC in straight sections, preventing sideslip is the key to driving safety in curved sections. This study takes the critical point at which vehicles slip at the design speed as the evaluation indicator, and uses CarSim/TruckSim simulation to obtain the threshold of DFC for curved road sections [19]. Based on the simulation results of this threshold, this study uses the DFC as the anti slip evaluation index to determine the timing of road surface anti slip recovery. Fig. 1 shows the decision-making process of preventive anti slip maintenance technology.

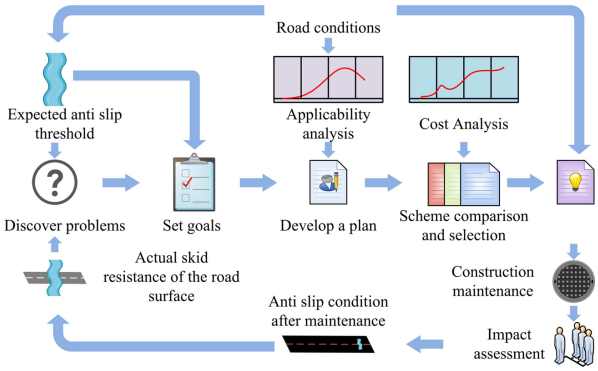

Fig. 1. Decision-making process of preventive anti-slip maintenance technology

3.2. Construction of Decision model for anti slip threshold and restoration technology of APS based on vehicle dynamics

The essence of neural networks can be treated as a composite function, which calculates the corresponding labels through the input of features. This is very consistent with the research on anti-skid maintenance decision-making, so BPNN is used to establish a decision-making model for asphalt pavement anti-skid recovery technology. Fig. 2 shows the algorithm flowchart for determining the timing of anti slip maintenance of asphalt pavement.

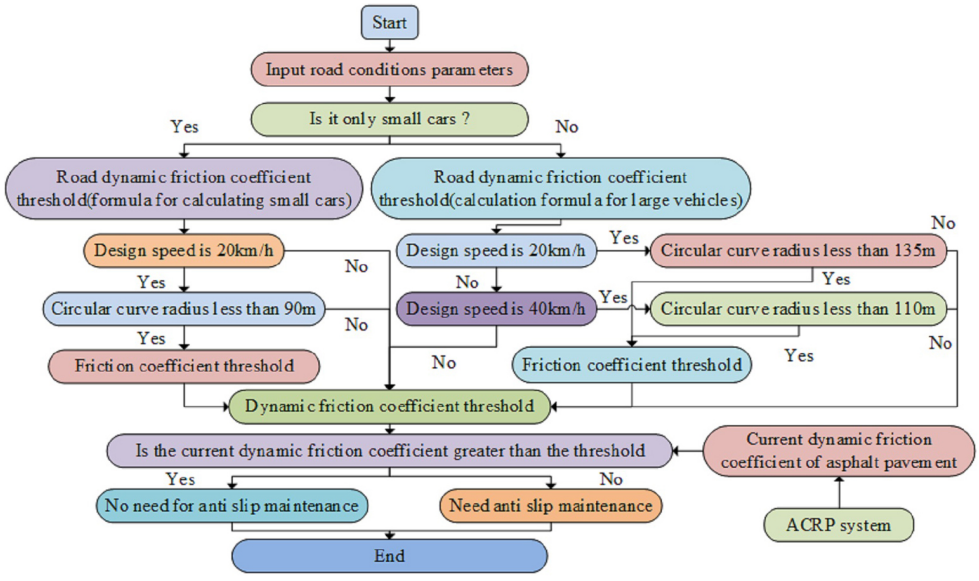

Fig. 2. Flow chart of timing decision algorithm for anti-skid maintenance of asphalt pavement

In Fig. 2, road condition parameters, such as road type and road slope, were first input into the asphalt pavement anti-skid maintenance timing decision model. Then select the driving model. If there is only a small car, the calculation formula of the small car is selected based on the design speed, and the threshold of the road friction coefficient is obtained by combining the longitudinal slope. If the design speed is 20 km/h and the radius of the circular curve is less than 95 m, the threshold of the dynamic friction coefficient is selected according to the elevation and longitudinal slope. Determine whether the current dynamic friction coefficient is greater than the threshold value. If it is greater than the threshold value, there is no virtual anti-skid repair; if it is less than the threshold value, anti-skid maintenance is required. Among them, the current dynamic friction coefficient is provided by asphalt pavement texture recognition ACRP system. Then output the result of the decision. If the design speed is 20 km/h and the radius of the circular curve is not less than 95 m, the threshold value of the dynamic friction coefficient is directly output, and then the judgment decision is made, and the judgment condition is unchanged. In addition, if the design speed is not 20 km/h, the threshold of dynamic friction coefficient is directly output, and the condition of anti-skid maintenance is judged to be unchanged. If there are more than small vehicles driving on the road, the calculation formula of large vehicles is selected according to the design speed, and the threshold of the road dynamic friction coefficient is obtained by combining the longitudinal slope. When the design speed is 20 km/h and the radius of the circle is less than 135 m, the threshold of the dynamic friction coefficient is selected according to the elevation and longitudinal slope, and the threshold of the dynamic friction coefficient is output, and the other judgment conditions remain unchanged. If the design speed is 40 km/h, but the radius of the circular curve exceeds 135 m, the threshold of the dynamic friction coefficient is directly output. In addition, if the design speed is 40 km/h and the radius of the circular curve is less than 110 m, the threshold of the dynamic friction coefficient is selected according to the elevation and longitudinal slope. If the design speed is 40 km/h, and the radius of the circular curve is not less than 110 m, the threshold of the dynamic friction coefficient is directly output. If the design speed is neither 20 km/h nor 40 km/h, the dynamic friction coefficient is directly output, and other judgment conditions remain unchanged. Error refers to the difference between the predicted value of any unit and the actual value, and its calculation is expressed in Equation (3.8).

$$\delta^{(3)} = Y^{(3)} - y^{(3)} = O_W(X) - y \tag{3.8}$$

After obtaining the error value of the output layer, the error of the hidden layer can be derived using Equation (3.9).

$$\delta^{(2)} = \left(W^{(2)}\right)\delta^{(2)} \cdot f'\left(p^{(2)}\right) \tag{3.9}$$

In Equation (3.9), $f'\left(p^{(2)}\right)$ represents the reciprocal of the excitation function. The sum of errors caused by weights is represented by $\left(W^{(2)}\right)\delta^{(2)}$. And through iterative operation, the optimal solution of the weight value is obtained. The neural network uses a loss function to represent the error between the predicted values of the model and the training samples. The study uses root mean square error as the loss function [20].

4. Experimental simulation analysis of decision model for anti slip restoration technology of APS

The typical vehicle dynamics software CarSim/TruckSim was used in the experiment to simulate the driving and braking safety processes of different types of vehicles under different driving road conditions, and the braking distance and whether the tire slid were used as evaluation indicators to judge the driving safety.

4.1. Effectiveness analysis of the decision model of anti-slip maintenance and restoration technology

When establishing BPNN, certain hyperparameters need to be manually set. When the quantity is too large, package the data into a certain number of batches and input them into the neural network to improve the calculation speed. This study sets the batch size to 32 and the learning rate lr to 0.1. The more learning rounds, the more accurate the model. Output loss every 50 rounds. Set the learning round to 4000 to ensure the accuracy of the model. After establishing the neural network, 70% of the sorted data is utilized as the training set, and the remaining is used as the test set. Calculate the loss and accuracy curve of the training and testing sets through the pyplot module in the Matplotlib library. Fig. 3 shows the loss and accuracy curve based on the anti slip recovery technology model.

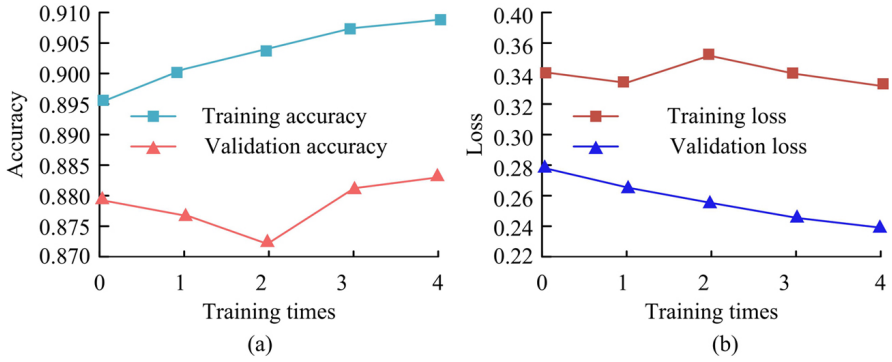

Fig. 3. Model loss and accuracy curves based on BP neural network; (a) Training and validation accuracy, (b) Training and validation loss

From Fig. 3, the training accuracy of the test set is stable at around 0.90, and the training loss value is around 0.34. This indicates that the model trained by BPNN has high accuracy and can be used for decision-making in anti slip recovery technology. 4 cases are entered in Table 1, with different and increasing design speeds. In each case, the number of vehicles on the road is not only limited to small cars, but the traffic flow is also increasing. Table 1 shows the relevant experimental parameters of the technical decision model for anti-skid maintenance and restoration of asphalt pavement.

Table 1. Experimental parameters of asphalt pavement anti-skid maintenance restoration technology decision model

Input parameter	Case 1	Case 2	Case 3	Case 4
V (km/h)	20	40	60	80
Traffic volume (10,000 vehicles)	60	800	1000	1200
Rainfall (mm)	560	350	1250	750
Original pavement type	AC	AC	AC	AC
Road slope (%)	5	4	3	2
Road radius (m)	10000	100	10000	10000
Road elevation (%)	0	6	0	0
Current DFC of pavement	0.36	0.20	0.36	0.36
Decision result	Unnecessary	Fine anti-slip gravel seal	Drained asphalt pavement	Table finishing

From Table 1, after all parameters are input into the model, the road dynamic friction coefficients obtained in Case 1, Case 2, Case 3 and Case 5 based on the research model are 0.36, 0.20, 0.36 and 0.36 respectively. The anti-skid recovery technologies corresponding to each case are unnecessary, fine anti-skid gravel sealing layer, drainage asphalt pavement, fine surface. This is consistent with the actual pavement anti-skid repair technology, which indicates that the decision of the model has a certain credibility. The experiment used the ACRP system to obtain three-dimensional point coordinate data of road surface texture. Fig. 4 shows the power spectral density and DFC variation curves of AC pavement under dry and humid conditions.

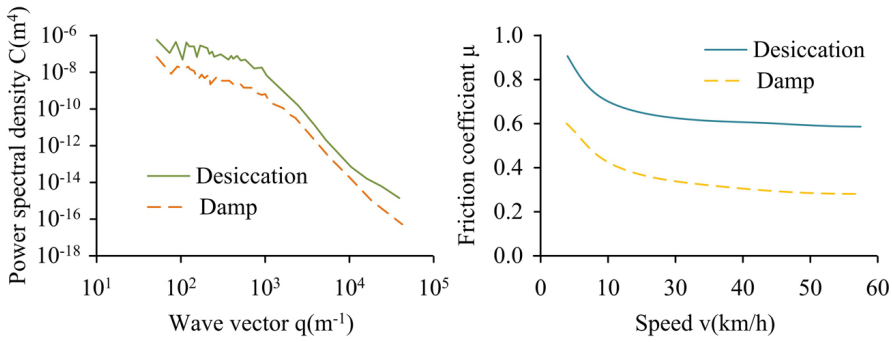

Fig. 4. Power spectral density and DFC of AC pavement under different states; (a) Power spectral density curve, (b) Dynamic friction coefficient change curve

From Fig. 4(a), under humid conditions, the power spectral density of AC road surface decreases at a faster rate. However, whether under wet or dry conditions, the trend of power spectral density changes on AC pavement is not significantly different. The fractal dimensions of road texture are roughly the same, and the self similarity characteristics remain unchanged. From Fig. 4(b), the skid resistance of the road surface under dry conditions is much higher than that of wet roads. The greater the speed, the more significant the difference. When the speed is 55 km/h, the DFC increases by 0.3059 compared to wet road surfaces.

4.2. Simulation and analysis of decision model of asphalt pavement anti-skid maintenance and restoration technology

This study uses typical vehicle dynamics software CarSim/TruckSim to simulate the driving and braking safety processes of different types of vehicles under different road conditions. The maximum braking distance is calculated using a safety factor of 0.95, and the maximum braking distance and the longitudinal driving distance of the vehicle from braking to the end of braking are shown in Fig. 5.

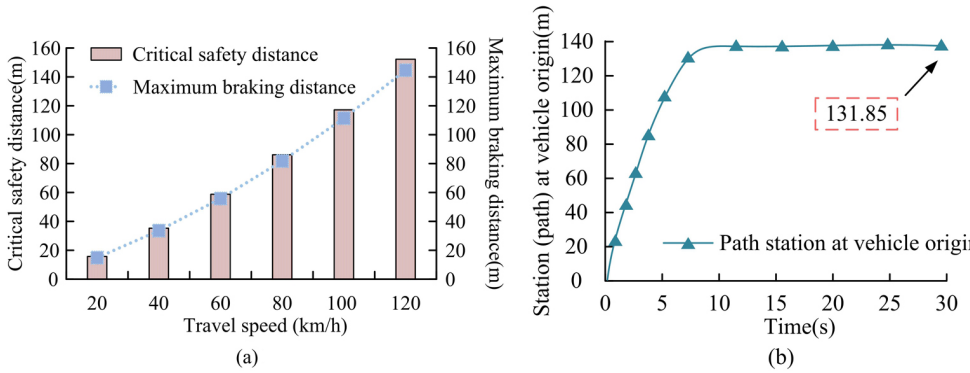

Fig. 5. Maximum braking distance and longitudinal driving distance of the vehicle from braking to the end of braking; (a) Maximum braking distance Recommended value, (b) Maximum braking distance in CarSim

In Fig. 5, as the driving speed increases, the critical safety distance and the maximum braking distance also increase. The path from the site to the vehicle origin is also increased. With the vehicle deviation exceeding 0.4 m as the criterion of sideslip and the critical point of sideslip occurring at the corresponding speed as the evaluation index, CarSim simulation was carried out to obtain the friction coefficient threshold of the road section. Fig. 6 shows the method for judging sideslip and rollover in CarSim.

From Fig. 6(a), the changes in the target and vehicle path of small and medium-sized vehicles simulated by CarSimf are almost consistent before the global X coordinate is 250 meters. Afterwards, the difference between the two increases with the increase of the X coordinate. From Fig. 6(b), the medium to large vehicles simulated by TruckSim are almost at the same lateral distance from the target path before the 8th to 9th seconds. Afterwards, the vehicle

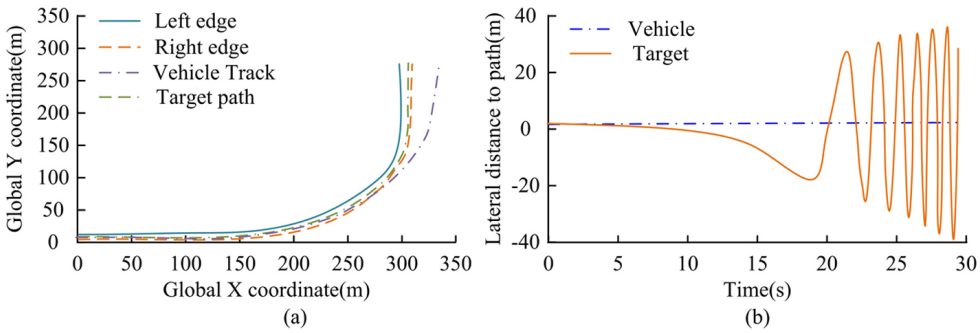

Fig. 6. CarSim middle side slide and rollover judgment method; (a) CarSim small car sideslip driving path, b) TruckSim rollover lateral migration curve of medium and large vehicles

rolled over and its lateral distance swing gradually increased. At the 30th second, the lateral distance between the vehicle and the target path is nearly –40 meters. Set the braking response time to 1 second, and in the simulation, the braking time and braking distance are calculated based on 2 seconds after driving to a stop. Fig. 7 shows the threshold values of DFCs for small and large vehicles on straight road sections at different design speeds.

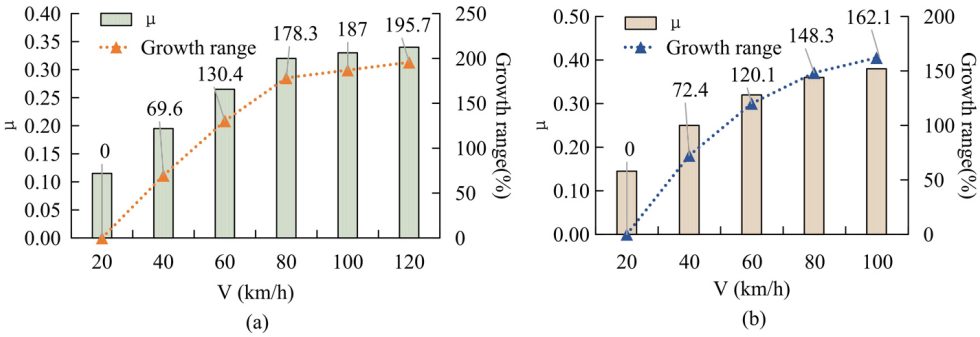

Fig. 7. Threshold values of DFC of linear road section for small vehicles and large vehicles at different design speeds; (a) Compact car, (b) Oversize car

In Fig. 7, compared to small cars, large cars have a higher demand for skid resistance on the road surface. When the speed is less than 60 km/h, the increase in μ is significant. The maximum difference in growth rate is 47.9%. When the speed exceeds 60 km/h, the increase in μ gradually slows down. Therefore, at lower speeds, it is more necessary to consider the variation value of the DFC. When the speed is high, more consideration needs to be given to its reference value. At the same speed, large vehicles have a higher μ value than small vehicles. When the speed is 40 km/h, the maximum difference between the two is 0.055. The required anti slip threshold for large cars is 28.21% higher than that for small cars.

5. Conclusions

To take real-time and effective preventive maintenance measures for the road in use, this study is based on the texture characteristics and vehicle dynamics theory of APS, and the decision model of APS anti-skid recovery technology based on the texture characteristics of the road is established. The simulation showed that the training accuracy of the test set was stable at around 0.90, and the training loss value was around 0.34. This indicated that the model trained by BPNN has high accuracy and can be used for decision-making in anti slip recovery technology. For large vehicles, the μ value increased from 0.145 to 0.38, an increase of 0.235. Compared to small cars, large cars had a higher demand for road surface skid resistance. When the speed was less than 60 km/h, the increase in μ value was significant. The maximum difference in growth rate was 47.9%. When the speed exceeded 60 km/h, the increase in μ value gradually slowed down. Therefore, at lower speeds, it was more necessary to consider the variation value of μ. When the speed was high, more consideration needed to be given to its reference value. At the same speed, large vehicles has a higher μ value than small vehicles. When the speed was 40 km/h, the maximum difference between the two was 0.055. The required anti slip threshold for large cars was 28.21% higher than that for small cars. Although this paper has achieved a high effect, due to the concentration of data sources, it also affects the breadth of decision making to a certain extent. Therefore, it is necessary to increase the effective proportion of data in the future.

References

[1] S. Purohit, M. Panda, and D.A. Kumar, "Performance of waste polyethylene modified bituminous paving mixes containing reclaimed asphalt pavement and recycled concrete aggregate", *Construction and Building Materials*, vol. 348, pp. 1–16, 2022, doi: 10.1016/j.conbuildmat.2022.128677.

[2] Z.X. Li, X.L. Shi, J.D. Cao, X.D. Wang, and W. Huang, "CPSO-XGBoost segmented regression model for asphalt pavement deflection basin area prediction", *Science China Technological Sciences*, vol. 65, pp. 1470–1481, 2022, doi: 10.1007/s11431-021-1972-7.

[3] G. Mazurek, P. Buczyński, and M. Iwański, "Stiffness modulus prediction against basic physical and mechanical characteristics of recycled base course with foamed bitumen and emulsified bitumen", *Archives of Civil Engineering*, vol. 69, no. 3, pp. 95–112, 2023, doi: 10.24425/ace.2023.146069.

[4] K. Yang and R. Li, "Characterization of bonding property in asphalt pavement interlayer: A review", *Journal of Traffic and Transportation Engineering (English Edition)*, vol. 8, no. 3, pp. 374–387, 2021, doi: 10.1016/j.jtte.2020.10.005.

[5] Z. Chen, "Research on internet security situation awareness prediction technology based on improved RBF neural network algorithm", *Journal of Computational and Cognitive Engineering*, vol. 1, no. 3, pp. 103–108, 2022, doi: 10.47852/bonviewJCCE149145205514.

[6] X. Wang, L. Gu, M.M. Dong, and X.L. Li, "State estimation of tire-road friction and suspension system coupling dynamic in braking process and change detection of road adhesive ability", *Proceedings of the Institution of Mechanical Engineers, Part D: Journal of Automobile Engineering*, vol. 236, no. 6, pp. 1170–1187, 2022, doi: 10.1177/09544070211035298.

[7] J. Hu, S. Rakheja, and Y. Zhang, "Tire-road friction coefficient estimation based on designed braking pressure pulse", *Proceedings of the Institution of Mechanical Engineers Part D Journal of Automobile Engineering*, vol. 235, no. 7, pp. 1876–1891, 2021, doi: 10.1177/0954407020983580.

[8] M. Furlan and G. Mavros, "A neural network approach for roughness-dependent update of tyre friction", *Simulation Modelling Practice and Theory*, vol. 116, art. no. 102484, 2022, doi: 10.1016/j.simpat.2021.102484.

[9] H. Pérez-Acebo, H. Gonzalo-Orden, D.J. Findley, and E. Rojí, "A skid resistance prediction model for an entire road network", *Construction and Building Materials*, vol. 262, art. no. 120041, 2020, doi: 10.1016/j.conbuildmat.2020.120041.

[10] M.G. Correia, T. de Oliveira e Bonates, B. de Athayde Prata, and E.F. Nobre Júnior, "An integer linear programming approach for pavement maintenance and rehabilitation optimization", *International Journal of Pavement Engineering*, vol. 23, no. 8, pp. 2710–2727, 2022, doi: 10.1080/10298436.2020.1869736.

[11] M. Mahmood, U. Anuraj, S. Mathavan, and M. Rahman, "A unified artificial neural network model for asphalt pavement condition prediction", *Proceedings of the Institution of Civil Engineers. Transport*, vol. 176, no. 1, pp. 14–24, 2023, doi: 10.1680/jtran.19.00111.

[12] H. Jing, P. Yao, L. Song, J. Zhang, Y. Zhao, and Z. Zhang, "Study of highway asphalt pavement recycling maintenance scheme decision system and decision method", *Journal of Intelligent and Fuzzy Systems*, vol. 43, no. 6, pp. 1–10, 2021.

[13] X. Wei, J. Chen, H. Gong, and Y. Sun, "Mesoscopic asphalt pavement response analysis using a random aggregate generation-based concurrent multiscale method", *Construction and Building Materials*, vol. 321, art. no. 126404, 2022, doi: 10.1016/j.conbuildmat.2022.126404.

[14] A. Emami, S. Khaleghian, and S. Taheri, "Asperity-based modification on theory of contact mechanics and rubber friction for self-affine fractal surfaces", *Friction*, vol. 9, pp. 1707–1725, 2021, doi: 10.1007/s40544-021-0485-5.

[15] S.H. Dong, S. Han, Q.X. Zhang, X. Han, Z. Zhang, and T.F. Yao, "Three-dimensional evaluation method for asphalt pavement texture characteristics", *Construction and Building Materials*, vol. 287, art. no. 122966, 2021, doi: 10.1016/j.conbuildmat.2021.122966.

[16] R. de Souze Sales, F.H.L. de Oliveira, and L. de Albuquerque Prado, "Performance of tire-asphalt pavement adherence according to rubber removal on runways", *International Journal of Pavement Engineering*, vol. 23, no. 10, pp. 3566–3576, 2022, doi: 10.1080/10298436.2021.1907577.

[17] A.J. Golrokh, X. Gu, and Y. Lu, "Real-time thermal imaging-based system for asphalt pavement surface distress inspection and 3D crack profiling", *Journal of Performance of Constructed Facilities*, vol. 35, no. 1, art. no. 04020143, 2021, doi: 10.1061/(ASCE)CF.1943-5509.0001557.

[18] C. Guo, X. Wang, L. Su, and Y. Wang, "Safety distance model for longitudinal collision avoidance of logistics vehicles considering slope and road adhesion coefficient", *Proceedings of the Institution of Mechanical Engineers, Part D: Journal of Automobile Engineering*, vol. 235, no. 2-3, pp. 498–512, 2021, doi: 10.1177/0954407020959744.

[19] X. Deng, Y. Zhang, and Y. Tang, "Investigation on slope rainfall threshold surface based on failure probablolity", *The Chinese Journal of Geological Hazard And Control*, vol. 32, no. 3, pp. 70–75, 2021, doi: 10.16031/j.cnki.issn.1003-8035.2021.03-09.

[20] L.J. Jobst, C. Heine, M. Auerswald, and M. Moshagen, "Effects of multivariate non-normality and missing data on the root mean square error of approximation", *Structural Equation Modeling: A Multidisciplinary Journal*, vol. 28, no. 6, pp. 851–858, 2021, doi: 10.1080/10705511.2021.1933987.

Received: 2023-10-16, Revised: 2023-12-28